Application of Arbitrary position and Width Pulse Train Signals in Ultrasonic Imaging

Linas SVILAINIS [1], Alberto RODRIGUEZ [2], Vytautas DUMBRAVA [1], Kristina LUKOSEVICIUTE [1], Arturas ALEKSANDROVAS [1], Dobilas LIAUKONIS [1]

[1] Kaunas University of Technology, Kaunas, Lithuania
Phone: +370 300532, Fax: + 837 324144; e-mail: linas.svilainis@ktu.lt
[2] Universidad Miguel Hernández de Elche Spain; E-mail: p. arodriguezm@goumh.umh.es

Abstract
Resolution of ultrasonic imaging demands wideband signals for excitation. If bandwidth improvement is done by reduction of the pulse duration signal to noise ratio is reduced. Spread spectrum signals allow increasing the signal energy and maintaining the resolution. Since signal frequency components are spread in time resolution is not reduced: such signals can be compressed using correlation processing. Chirp signals are most widely used, but suffer high correlation sidelobes. Arbitrary position and width pulse (APWP) trains are a novel class of spread spectrum signals. Spectral spread is produced using trains of rectangular pulses which are placed at specific positions in time in order to provide a spectrum spread of the signal. It is expected that APWP should have properties of chirp (wideband and compressible) and of a single pulse (low correlation sidelobes). Usually signal envelope is used in imaging. Then signal possessing lowest sidelobes of the correlation envelope are of interest. But in such case accuracy of signal detection is significantly reduced because it's envelope bandwidth which determines the attainable random errors. Aim of the investigation was the RF sidelobes of the signals discussed. Optimization of the signals was carried out to achieve the lowest RF correlation sidelobes. Experimental investigation results of APWP signals comparison with conventional signals are presented.

Keywords: ultrasonic imaging, arbitrary position and width pulse train signals, spread spectrum signals, ultrasonic signal processing.

1. Introduction

Rectangular pulses are the usual choice for ultrasonic transducer excitation. Temporal resolution of ultrasonic imaging requires wideband signals. Signal to noise ratio is reduced if improvement of the bandwidth is done by reduction of the pulse duration. Signal energy can be improved by increasing the amplitude of the excitation pulse. Amplitude can reach 800 V [1,2]. Higher amplitude means the reduction of the probing signal's bandwidth: rise and fall fronts are longer because slew rate of the pulser is almost constant [3]. Also larger amplitude is causing higher nonlinear distortions in the propagation path [4]. Besides, single rectangular pulse has its energy concentrated at low frequencies and has spectral zeroes. Spread spectrum (SS) signals allow increasing the signal energy and maintaining the resolution [5,6]. Resolution is not reduced since signal frequency components are spread in time: such signals can be compressed using correlation processing. The bandwidth of the ultrasonic system is limited by the ultrasonic transducer used so is the achievable resolution. But with a proper spread spectrum signal this bandwidth can be exploited to its maximum even for narrowband case [7]. Unfortunately, compression of such signal produces a small leak of the signal energy into sidelobes which in turn reduces the attainable contrast of the image. That's why such wide variety of spreading techniques was developed [7-13] with different advantages of the each. Arbitrary waveform signals [13] are attractive since any suitable signal shape can be produced. But this introduces high complexity of system electronics which increases the system size and cost. Our research is aimed at exploring just rectangular, binary signals (unipolar or bipolar). Then output stage complexity is drastically reduced. Chirp signals are most widely used [11,13]. These offer spectral content control, can use binary excitation signals but suffer high correlation sidelobes [12]. Phase coded sequences are another type of the spread spectrum signals [8,9]. Here, radio frequency (RF) signal phase is manipulated

according to code. Main advantage of these signals is that binary signals can be used for excitation. Phase coded sequences offer little bandwidth control even if fractional phase is used. Arbitrary position and width pulse (APWP) trains are a novel class of spread spectrum signals. Spectral spread is produced using trains of rectangular pulses which are placed at specific positions in time in order to provide a spectrum spread of the signal. It is expected that APWP should have properties of chirp (wideband and compressible) and of a single pulse (low correlation sidelobes). Aim of this work was to compare the performance of the most popular signals with APWP.

2. Aim of the investigation

Random errors of the time-of-light (ToF) position estimation are defined by the signal to noise ratio (SNR) and the effective signal bandwidth F_e [14,15]:

$$\sigma(TOF) \geq \frac{1}{2\pi F_e \sqrt{SNR}}, \; SNR = \frac{2E}{N_0}, \quad \text{..... (1)}$$

where F_e is a squared sum of envelope bandwidth β and center frequency f_0:

$$F_e^2 = \beta^2 + f_0^2, \; \beta^2 = \frac{\int_{-\infty}^{\infty} (f - f_0)^2 |S(f)|^2 df}{E}, \; f_0 = \frac{\int_{-\infty}^{\infty} f |S(f)|^2 df}{E}, \quad \text{..... (2)}$$

Quality of the image obtained using ultrasonic signals is not directly influenced by SNR, but manly depends on the sharpness of the signal which in turn can be related to the envelope bandwidth β. Imaging systems usually explore the envelope of the signal for image production [13]. Therefore research of the signal correlation sidelobes is mainly targeted for envelope sidelobes reduction.

Spread spectrum signals have the advantage of high energy and compressibility but suffer high correlation sidelobes [7,12,13]. High signal to noise ratio (SNR) counters with correlation sidelobes therefore image contrast is reduced. Application of nonlinear frequency modulation signals allows controlling the shape of the spectrum and the sidelobe level [11]. Correlation function of the 13 element Barker code is presented below (figure 1) before passing this signal through the system.

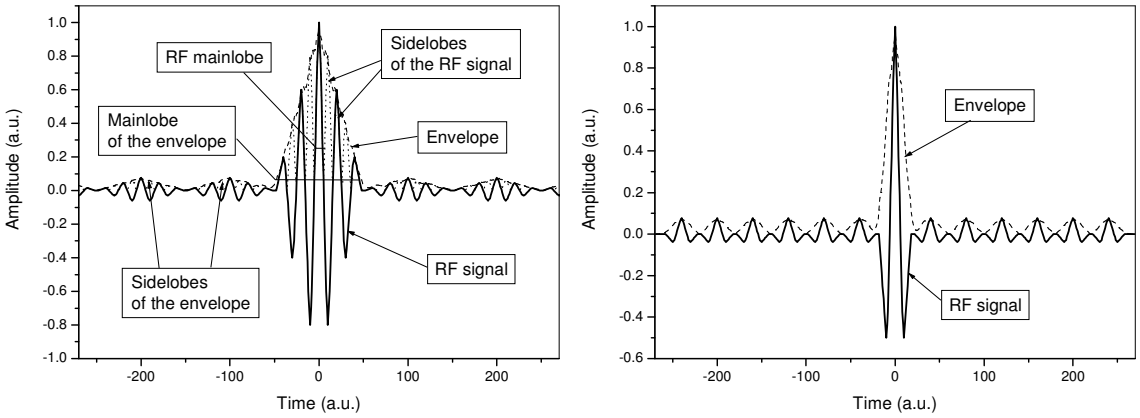

Figure 1. Autocorrelation function of the Barker 13 code with chip size 2.5 periods (left) and 1 period (right)

It can be seen, that Barker code is used to encode the phase of the CW toneburst, therefore only envelope is following the expected code properties (sidelobe level is -22.3 dB for envelope only). Applying equation (2) on signal in figure 1 left we obtain that F_e is 4.8 MHz for RF signal, while using the envelope F_e bandwidth is only 0.5 MHz. This means that

random errors will increase 10 times when using the envelope instead of the RF of the cross-correlation function. Of, course, it is possible to reduce the chip size down to 1 period (figure 1 right) but in such case F_e of the envelope is 0.7 MHz (increase of random errors of ToF estimation 7 times).

Low correlation sidelobes of the RF, not the envelope of the signal, are demanded if iterative deconvolution is used to disassemble the A-scan signal into train of pulses [16]. Here it is important to have the RF mainlobe as narrow as possible and keep the correlation sidelobes minimal.

If reduction of the RF sidelobes is necessary, then it is equivalent to reducing the width of the mainlobe width of the envelope. This in turn is equivalent to increasing the signal bandwidth. But the ultrasonic transducer is limiting the bandwidth of the signal. Then, signal with bandwidth compensation is needed. This can be accomplished by the bandwidth loss compensation after signal is received. Deconvolution [17,18] is the usual approach for bandwidth improvement. But increasing the frequency components which have been attenuated increases the noise level. Therefore better approach is to alter the frequency content of the probing signal so more energy is placed at the components that will be attenuated [1]. The investigation below was aimed to decide which signal types are suited for such signal optimization.

3. Selection of candidate signals

Spherically focused 60 % bandwidth 5 MHz center frequency ultrasonic transducer IRY405 from NDT transducers PLL was chosen for investigation. Excitation was performed using a unipolar pulser, capable of rectangular pulses production [3]. Selection of the signals was based on the system frequency response which was obtained using linear, 1-10 MHz, 6 µs, duration, 15 V amplitude chirp and 10 dB gain of the preamplifier. In order to compare the signals under the same conditions and speed up the optimization process, initial analysis was carried out digitally, using system transmission response *TT* and signal code C_i in Matlab. Reflection from stainless steel slab (figure 2 left) was taken as reference.

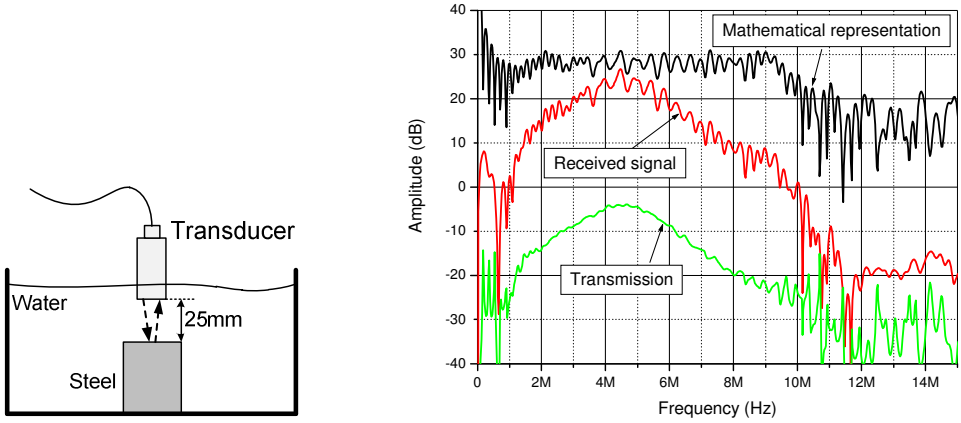

Figure 2. Setup to acquire the system response (left) and obtained frequency response of the transmission (right)

Transmission of the system *TT* was obtained by taking the ratio of the forward Fourier transforms (FFT) of the signal reflected from the stainless steel slab *RX* and the mathematical representation of the excitation code C_{chirp}:

$$TT(\omega) = \frac{FFT[RX(t)]}{FFT[C_{chirp}(t)]}, \quad (3)$$

With system model and signal i code C_i available expected system response RX_i (signal which suppose to appear at the output of transducer) was obtained by multiplication in frequency domain ant transfer into time domain by inverse Fourier transform (IFT):

$$RX_i(t) = IFT\{FFT[C_i(t)] \cdot C_{chirp}(\omega)\}, \quad (4)$$

All signals considered were unipolar rectangular pulses with amplitude 15 V. All spread spectrum signals were 3 μs duration in order to equalize the amount or initial energy. Three types of rectangular pulse signal were chosen: i) 50 ns duration (representing spike excitation); ii) 120 ns duration (representing best excitation) and iii) 220 ns duration (best RF sidelobe to mainlobe level ratio). In essence desired signal should provide a spectral dip at transducer center frequency increasing the resulting signal bandwidth [1] so type iii) pulse corresponds to such case. Two types of CW toneburst signals were used: i) 4.5 MHz (representing best excitation); ii) 7.45 MHz (representing lowest sidelobes and shortest RF mainlobe). Three types of chirp signal were selected: i) linear 3 μs duration chirp 1 MHz to 10 MHz (representing classical chirp where spectral shaping occurs naturally thanks to transducer frequency response); ii) linear 3 μs duration chirp 1 MHz to 5 MHz (best RF sidelobe to mainlobe level ratio) and iii) nonlinear 3 μs duration chirp generated using adaptive 4-th order polynomial for instantaneous frequency generation (best RF sidelobe to mainlobe level ratio). RF sidelobe to mainlobe level ratio optimized APWP signal [7] with 3 μs duration was selected as the representative of the type where there is most of the flexibility in signal shape. Last type selected was 13 elements Barker code, as a representative of spread spectrum signals where control of the spectral shape is not possible. Main signal parameters are presented in table 1.

Table 1. Parameters and properties of the excitation signals used in investigation

Label	Signal type	Parameters	SLL_{RF} dB	SLL_{Henv} dB	τ_{RF} ns	E_i dB	F_e MHz	β MHz
P50	Pulse	50ns	-3.1	-22	73	0	4.9	2.0
P120	Pulse	120ns	-3.3	-22	85	6	4.2	1.7
P220	Pulse	220ns	-7.6	-22	108	4	3.7	2.3
CW5	CW toneburst	4.5 MHz, 3 μs	-0.3	-31	74	19	4.6	0.8
CW7	CW toneburst	7.45 MHz, 3 μs	-3.6	-7.1	53	7	7.1	4.0
Ch10	Linear chirp	1-10 MHz, 3 μs	-3.7	-13.7	74	14	4.9	2.2
Ch5	Linear chirp	1-5 MHz, 3 μs	-2.6	-14.9	87	16	4.1	1.6
NLch	Nonlinear chirp	3 μs duration	-13.1	-11.3	106	10	3.9	2.6
APWP	APWP	3 μs duration	-15.1	-10.7	103	10	4.0	2.7
B13	Barker code 13	chip=1 period	-2.5	-18.0	78	16	4.5	1.7

Obtained signals were compared by the level of the correlation RF sidelobes, correlation envelope sidelobes, mainlobe duration, energy, effective bandwidth and envelope bandwidth. RF sidelobe to mainlobe level ratio was calculated by taking the peak P_0 and peak RF sidelobe P_{SL} outside the main peak of the autocorrelation function R (refer figure 1):

$$SLL_{RF} = 20\lg\frac{\max[R\{RX_i(t)\}]}{\max[R\{RX_i(t)\}]_{t\neq\pm 0.5\tau_{RF}}}, \quad (5)$$

Envelope sidelobe to mainlobe level ratio was calculated by taking the peak P_{0E} and peak RF sidelobe P_{SLE} outside the main peak of the autocorrelation function R (refer figure 1). Envelope was obtained using Hilbert transform and taking the magnitude of the result:

$$SLL_{Henv} = 20\lg\frac{\max\left[\left|Hilb\left(R\{RX_i(t)\}\right)\right|\right]}{\max\left[\left|Hilb\left(R\{RX_i(t)\}\right)\right|\right]_{t\neq\pm 0.5\tau_{RF}}}, \quad (6)$$

RF mainlobe duration τ_{RF} was obtained at 0.5 level of the peak P_0:

$$\tau_{RF} = \arg\left(R\{RX_i(t)\} = 0.5P_0|_{t>0}\right) - \arg\left(R\{RX_i(t)\} = 0.5P_0|_{t<0}\right), \quad (7)$$

Signal energy E_i was evaluated without taking the impedance into account and then normalized by the energy $E_{pulse50ns}$ of the shortest rectangular pulse used:

$$E_i = \frac{\int_{-\infty}^{\infty}|RX_i(t)|^2 dt}{\int_{-\infty}^{\infty}|RX_{pulse50ns}(t)|^2 dt}, \quad (8)$$

Totally 10 signals were selected for analysis. Properties obtained using simulated system transmission and main signal parameters are presented in figures 3, 4 and 5 below.

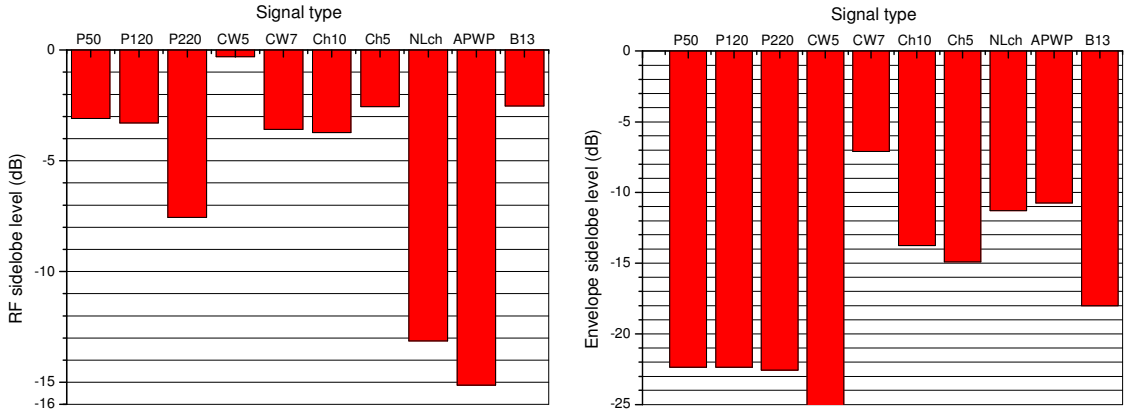

Figure 3. Signal correlation sidelobes level vs. signal type: RF (left) and envelope (right)

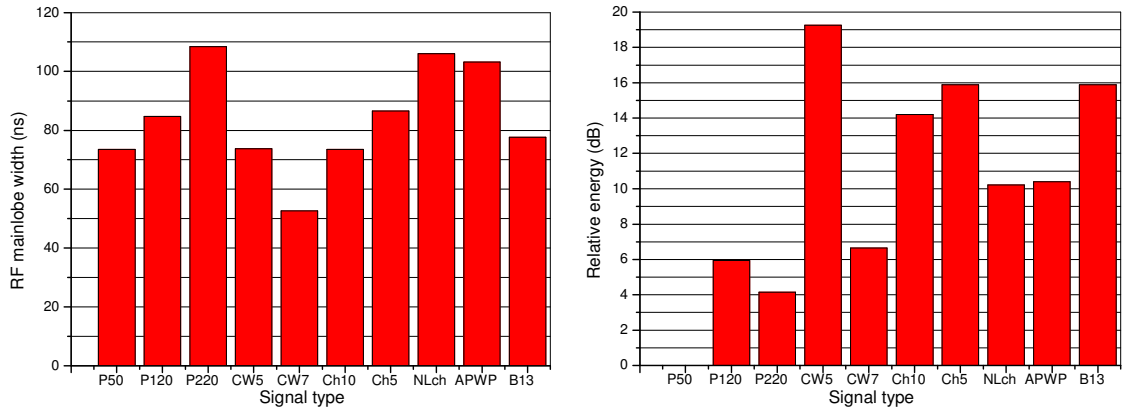

Figure 4. Signal RF correlation mainlobe width (left) and relative energy (right) vs. signal type

Analysis presented above indicates that APWP and nonlinear chirp signals have lowest RF correlation sidelobes level. Price for such improvement is significant loss of energy: it's only 10dB higher that pulse. As it comes to envelope sidelobes, pulse and CW toneburst signals indicate best results. But this assumption is misleading: these signals are not compressible therefore sidelobes do not exist. Barker code indicated lowest envelope sidelobes, but -18 dB instead of expected -22.3 dB. Envelope sidelobes are 8 dB worse for APWP and nonlinear chirp but these signals were not optimized for the envelope sidelobes. As expected, narrowest mainlobe was detected for 7.45 MHz CW toneburst signal: despite being away from the

center frequency, it has enough energy to produce the narrow mainlobe, but it has very high sidelobe level and low energy, almost same as pulse.

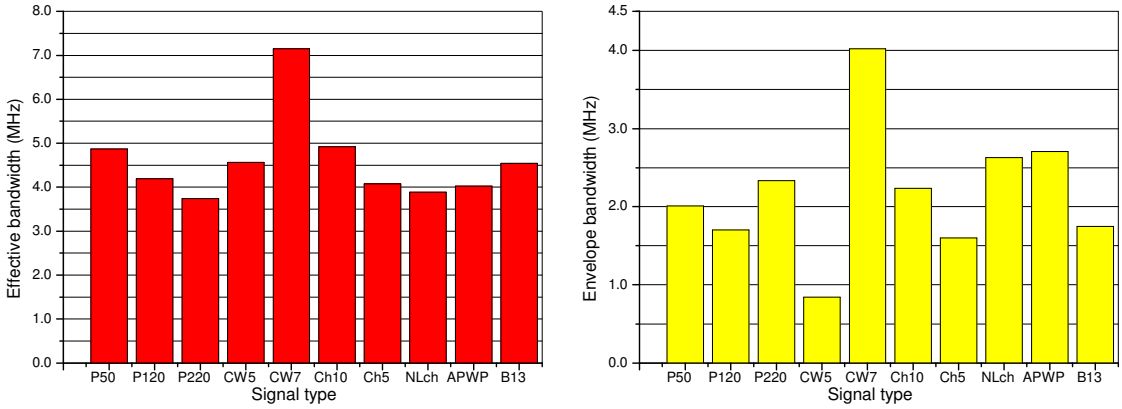

Figure 5. Effective bandwidth (left) and envelope bandwidth (right) of the signal

Analyzing figure 5 one may conclude that 7.45 MHz CW toneburst signal has best effective bandwidth. Rests of the signals have comparable effective bandwidth. This is natural to expect since effective bandwidth is constructed mainly by center frequency. It is worth to note that APWP and nonlinear chirp signals together with 7.45 MHz CW toneburst and 220 ns pulse have widest envelope bandwidth. Therefore range resolution of these signals should be the best. But it must be taken into account that energy is low for 7.45 MHz CW toneburst and 220 ns pulse.

4. Experimental investigation results

With the set of optimized signals available, real world experiments have been carried out. Emulated situation (figure 6) was representing small defect present close to the backwall of the test sample. Defect was emulated by the 0.34 mm diameter fishing line placed above the thick Plexiglas slab.

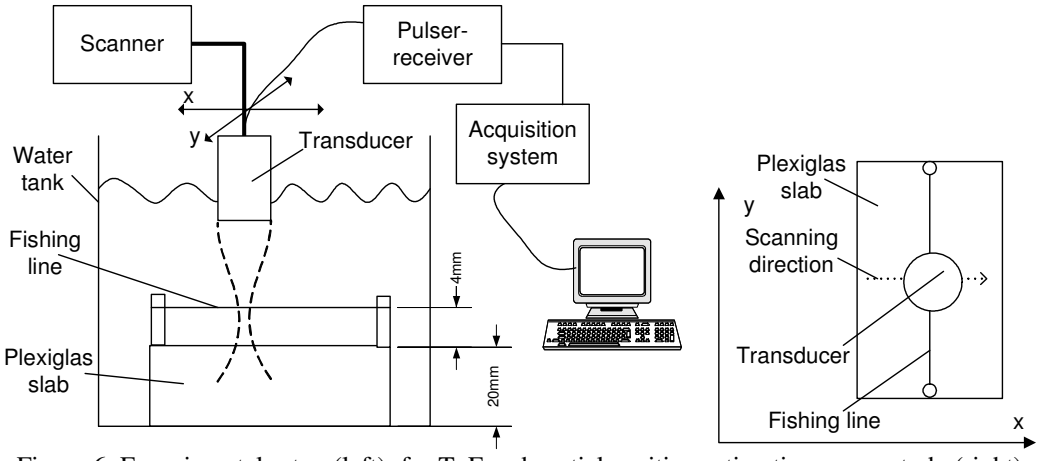

Figure 6. Experimental setup (left): for ToF and spatial position estimation errors study (right)

Same spherically focused 5 MHz ultrasonic transducer IRY405 from NDT transducers PLL was used. Excitation was performed using same unipolar pulser using 15 V excitation signal amplitude and 12 dB gain of the preamplifier. Signal was always acquired with large refection from the Plexiglas present, so gain and the excitation amplitude were adjusted according to this signal. Therefore signal from fishing line was considerably smaller.

4.1 Random errors of Time of Flight estimation and signal to clutter ratio study

This experiment was aimed to evaluate the random errors of the defect temporal position estimation. Fishing line was placed at 4 mm from the Plexiglas slab (figure 6, left). Transducer was precisely positioned above the fishing line at focal distance - 37 mm. A-scan signals were acquired 1000 times in same position. Obtained data was aligned and averaged to produce the reference signal which later was used for Time of Flight (ToF) calculation. Temperature of the bath was not controlled therefore temperature variation induced a trend in the measurements. Moving average filter of 20 samples was used to smooth the data. After removing the trend from the ToF array, standard deviation of the ToF was calculated. Comparison of random errors for ToF estimation (when RF and envelope of the correlation are used) are summarised in figure 7.

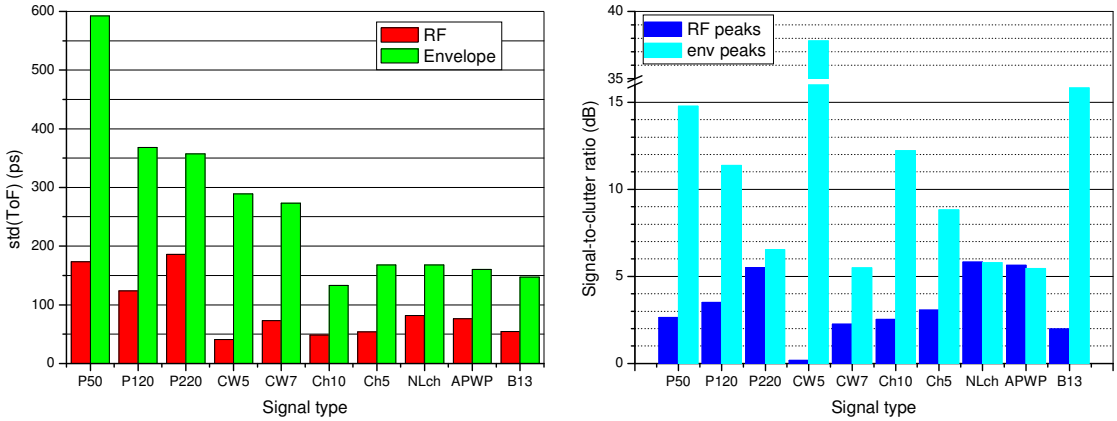

Figure 7. Random errors of ToF estimation (left) and signal to clutter ratio in time domain (right)

It can be seen that lowest random errors are in case of RF information exploitation. Best performance was for CW toneburst with the frequency matching the transducer response. Errors for spread spectrum signals are low for both in case of RF and envelope information thanks to high energy. Additionally, signal to clutter ratio (SCR) was calculated using peak values (figure 7 right). In case of envelope SCR was highest for CW toneburst with the frequency matching the transducer response but this conclusion is misleading since mainlobe of the correlation envelope for this signal is very wide. Barker code and short pulse have best performance here. Best performance for RF case was for nonlinear chirp and APWP signal.

4.2 Spatial position estimation random errors study

This experiment was aimed to evaluate the random errors of the defect spatial position estimation. Fishing line was placed at 4 mm from the Plexiglas slab (figure 6, right) and one line along coordinate x scanned across the fishing line using 10 nm step. One hundred A-scans were acquired at every scanner position. This data was later split to emulate the situation where same scan along x axis which was carried out 100 times. This one hundred scanner positions was used to locate the position x_{peaki} where signal reflected from fishing line has maximum value, assuming it as a defect spatial position. Both raw data and the cross-corelation result were used for maximum location. Obtained data positions x_{peaki} were processed to obtain the random errors (standard deviation) of this position estimation. Results are summarised in figure 8, left. It can be seen that lowest random errors are for CW toneburst of the frequency matching the transducer center frequency. Random errors are small for spread spectrum signals too.

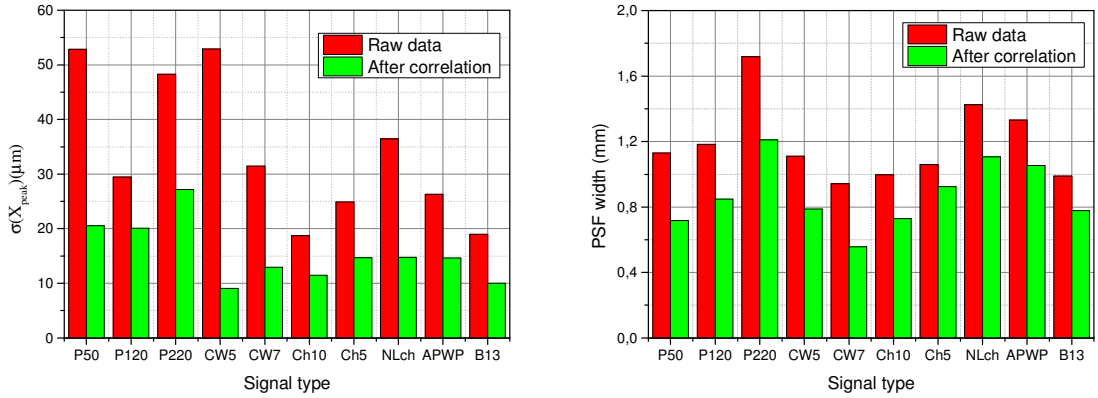

Figure 8. Random errors of spatial position estimation (left) and PSF width @-6dB (right)

Same data was averaged and later used to produce the point spread function (PSF) at -6dB level. Comparison of PSF width for all signal types is presented in figure 8, right. It can be seen that narrowest PSF is for 7.45 MHz CW toneburst signal: it has highest amount of energy at high frequencies. Spread spectrum signals performance is comparable to that of the pulse signals.

5. Conclusions

The aim of investigation was to decide which signal types are suited for signal optimization to achieve the lowest RF correlation sidelobes. It was demonstrated that APWP signals are attractive since any desired RF signal shape can be produced: these signals had lowest RF sidelobes. APWP and other spread spectrum signals had similar performance in random errors of temporal position estimation. APWP performance in spatial domain was lower than for other signals due to the energy losses. Artificially offset frequency (7.45 MHz instead of 5MHz) CW toneburst produced best spatial resolution. Barker code 13 with chip size 1 period and 5MHz CW toneburst allowed for lowest spatial position estimation errors thanks to high energy.

Acknowledgements

This research was funded by a grant (No. MIP-058/2012) from the Research Council of Lithuania.

References

1. J Salazar, et al. High-Power High-Resolution Pulser for Air-Coupled Ultrasonic NDE Applications', IEEE Trans. Instrum. Meas, Vol 52, No 6, pp 1792 – 1798, 2003.
2. L Svilainis, V Dumbrava, A Chaziachmetovas, A Aleksandrovas, 'Pulser for Arbitrary Width and Position Square Pulse Trains Generation,' IEEE international ultrasonics symposium (IUS), 2012
3. L Svilainis, A Chaziachmetovas, V Dumbrava, 'Efficient high voltage pulser for piezoelectric air coupled transducer', Ultrasonics, Vol 53, No 1, pp 225-231, 2013.
4. M A Averkiou, M F Hamilton, 'Nonlinear distortion of short pulses radiated by plane and focused circular pistons', Acoustical Society of America, Vol 102, No 5, pp 2539-2548, November 1997.

5. L R Welch, M D Fox, 'Practical spread spectrum pulse compression for ultrasonic tissue imaging', IEEE Trans. Ultrason. Ferroelect. Freq. Control, Vol 45, No 2, pp 349-355, March 1998.
6. A Kasaeifard, J Saniie, 'A successive parameter estimation algorithm for chirplet signal decomposition', IEEE international ultrasonics symposium (IUS), pp 1465-1468, 2012.
7. L Svilainis, A Aleksandrovas, 'Application of arbitrary pulse width and position trains for the correlation sidelobes reduction for narrowband transducers', Ultrasonics, Vol 53, No 7, pp 1344-1348, September 2013.
8. Z Haichong, et al., 'Simultaneous Multispectral Coded Excitation Using Periodic and Unipolar M-sequences for Photoacoustic Imaging', Conference on Photons Plus Ultrasound - Imaging and Sensing Location, Vol 8581, 2013.
9. C Xiaodong, et al., 'Increasing average power in medical ultrasonic endoscope imaging system by coded excitation', International Conference on Optical Instruments and Technology, Vol 7156, 2009.
10. C H Hu, et al., 'Coded excitation using biphase-coded pulse with mismatched filters for high-frequency ultrasound imaging', Ultrasonics, Vol 44, pp 330–336, 2006.
11. M Pollakowski, H Ermert, L von Bernus, T Schmeidl, 'The optimum bandwidth of chirp signals in ultrasonic applications', Ultrasonics, Vol 31, No 6, pp 417-420, 1993.
12. T Virolainen, J Eskelinen and E Haeggstrom, 'Frequency Domain Low Time-Bandwidth Product Chirp Synthesis for Pulse Compression Side Lobe Reduction', IEEE international ultrasonics symposium (IUS), pp 1526 - 1528, 2012.
13. T Misaridis and J A Jensen, 'Use of Modulated Excitation Signals in Medical Ultrasound. Part II: Design and Performance for Medical Imaging Applications', IEEE Trans. Ultrason. Ferroelect. Freq. Control, Vol 52, No 2, pp 192-207, March 2005.
14. H Cramer, 'Mathematical Methods of Statistics', Princeton Univ. Press. 1946.
15. C Rao, 'Information and the accuracy attainable in the estimation of statistical parameters', Bulletin of Calcutta Mathematics Society, Vol 37, pp 81-89, 1945.
16. L Svilainis, A Aleksandrovas, K Lukoseviciute, V Eidukynas, 'Investigation of the Time of Flight Estimation Errors Induced by Neighboring Signals', IEEE IDAACS, pp 413-418, 2013.
17. S Kageyama, H Hasegawa, H Kanai, Hiroshi, 'Increasing Bandwidth of Ultrasound Radio Frequency Echoes Using Wiener Filter for Improvement of Accuracy in Measurement of Intima-Media Thickness', Japanese journal of applied physics, Vol 52, No 7, pp 07HF04-1-6, July 2013.
18. F Honarvar, H Sheikhzadeh, M Moles, A N Sinclair, 'Improving the time-resolution and signal-to-noise ratio of ultrasonic NDE signals', Ultrasonics, Vol 41, pp 755-763, 2004.